

Wet skid resistance · silica, coupling agent · filler-polymer interaction · loss angle

Changes in the coupling agent structure in a silica-silane filler system lead to alterations of the microstructure of the silica-polymer interface and determine the dynamic properties, thus wet skid resistance (WSR) and rolling resistance (RR) of a tire tread. Silanes with one ethoxy-group instead of three decrease the hysteresis at 6 °C and increase it at low temperatures, indicating improved RR as well as WSR. A longer linker lowers the hysteresis at elevated temperatures. Lack of chemical coupling between filler and polymer results in a drop in WSR as well as an increase of RR. This implies that simple hydrophobation of the silica surface is not sufficient to obtain good WSR and RR.

Einfluss der Mikrostruktur von Kieselsäure-Polymer-Bindungen auf die Reifenleistungsfähigkeit-Indikatoren

Nasshaftung · Kieselsäure · Silanko · Polymer-Füllstoff Wechselwirkungen · Verlustwinkel

Die molekulare Struktur der Silane in einer Kieselsäure-Mischung bestimmt die Mikrostruktur der Füllstoff/Polymer-Grenzfläche und somit die dynamischen Eigenschaften. Dieses ist maßgebend für reifenspezifische Eigenschaften wie Rollwiderstand und Nasshaftung. Silane mit nur einer Ethoxy-Gruppe verringern die Hysterese bei 60 °C und erhöhen diese bei niedrigen Temperaturen und sind Indikatoren für Rollwiderstand und Nasshaftung. Der Ersatz der Propyl- durch eine größere Alkylgruppe führt zur Verringerung der Hysterese bei höheren Temperaturen. Ein Silan ohne Bindungsmöglichkeit zum Polymer beeinflusst Rollwiderstand und Nasshaftung negativ.

Figures and Tables:
By a kind approval of the authors.

Influence of Silica-Polymer Bond Microstructure on Tire-Performance Indicators

Introduction

Because of a reduced rolling resistance (RR) and improved wet skid resistance (WSR), tire treads of passenger cars are nowadays almost exclusively produced in Europe by the use of silica technology. The key element in this technology is the coupling agent, a silane, which chemically couples silica to the polymer. The chemical structure of the silane determines the polymer-filler interactions, which on their turn influence wet skid and rolling resistance. The goal of the present study is to characterize the underlying mechanisms involved in rubber-filler interactions for the wet skid resistance of tires, a dynamic viscoelastic phenomenon.

To characterize the dynamic properties of rubber, storage and loss moduli are commonly measured. The ratio of loss to storage modulus is indicated as the $\tan \delta$. In order to elucidate the mechanisms responsible for WSR, a first approach is based on increasing the interaction between filler and polymer. This leads to improvement of wet skid resistance by raising the $\tan \delta$ values in the low temperature region (0 - 20 °C) and decreasing the same in the higher temperature region [1]. Based on the time-temperature superposition, increased hysteresis at lower temperatures should increase energy dissipation at higher frequencies, occurring during wet skidding. A second approach is that the filler-polymer interaction should be limited ultimately to physical interactions. Physical interaction means that under the influence of energy resulting from skidding, polymer molecules can easily be displaced on the filler surface, what should increase energy dissipation. These two approaches are obviously contradicting.

The investigation of the above mentioned phenomena and their effect on the dynamic properties requires on one hand the use of silanes without the ability of coupling to the polymer: (bis-(triethoxysilyl)hexane). On the other hand, in order to induce stronger polymer-filler interactions than the commonly used silane with three ethoxy groups (bis-(triethoxysilylpropyl)tetrasulfide) can provide, a

coupling agent with only one silica-silane bonding unit (bis-(dimethylethoxy-silylpropyl)tetrasulfide) is applied [2]. In this case, replacing two out of three ethoxy groups by methyl moieties leads to less bulky silane molecules, hence more silane molecules can attach to the silica surface and lead to a higher bond density with the polymer chain. In fact just one ethoxy group is necessary to make the bond between a silanol group on the silica surface and a polymer chain. A silane with a longer linker between the silyl-group and the sulfur-moiety (bis-(triethoxysilyldecyl)tetrasulfide) is applied to make the silica-rubber interphase more flexible, but still with a chemical bond to the polymer chain. The interphase structure obtained by use of this silane is in-between the strong interactions of the chemical bond of the propyl-silane, and the weak interactions due to the increased flexibility of the longer linker.

The practical laboratory assessment methods for wet skid resistance for carbon black filled compounds indicate that higher values of $\tan \delta$ at lower temperatures, preferably between 0 °C to 20 °C, correspond to better wet skid resistance of a tire tread [3,4]. The frequency of a rolling tire is around 10 Hz; however, when the tire stops its rotation and starts skidding, the frequency rises up to the megahertz region. This high frequency is the result of stick-slip phenomena during skidding [5]. The service tempera-

Authors

Ernest Cichomski, Anke Blume, Wilma K. Dierkes, Jacques W.M. Noordermeer, Tanya V. Tolpekina, Steven Schultz, Enschede, the Netherlands

Corresponding author:
Jacques W.M. Noordermeer
University of Twente, Dept. of
Elastomer Technology and Engineering,
P.O. Box 217, 7500 AE
Enschede, the Netherlands
j.w.m.noordermeer@utwente.nl



KGK RUBBERPOINT

Discover more interesting articles
and news on the subject!

www.kgk-rubberpoint.de



Entdecken Sie weitere interessante
Artikel und News zum Thema!

| I Chemical structures of silanes | | |
|----------------------------------|--|--------------------|
| No. | Compoundname | Chemical structure |
| I | Bis-(triethoxysilylpropyl)tetrasulfide, (TESPT) MW = 532 g/mol. | |
| II | Bis-(dimethylethoxysilylpropyl)tetrasulfide, (DMESPT) MW = 418 g/mol. | |
| III | Bis-(triethoxysilyl)hexane, (TESH) MW = 410 g/mol. | |
| IV | Bis-(triethoxysilyl)tetrasulfide, (TESDeT) MW = 734 g/mol. | |

ture of a tire during rolling is relatively high: around 50 - 60°C. Based on the time-temperature superposition principle, the $\tan \delta$ curve shifts towards higher temperatures under the influence of increasing frequencies: the values of $\tan \delta$ at low frequencies and at 0 - 20°C are shifted by the high frequencies to the range of the service temperatures of tires [6, 7]. Hence, rubbers which loose more

energy in the low temperature range should have a higher wet skid resistance. The influence of the silica-polymer interphase structure on wet skid performance was investigated by testing the dynamic properties, in particular the $\tan \delta$ in the temperature range from 0 - 20°C at 10 Hz. The values of the loss angle in this temperature range are so far the most suitable indicators for the

wet skid performance of a tire tread [8]. However, a WSR indicator closer to actual practice are measurements on a Laboratory Abrasion Tester 100 (LAT 100) on which additional measurements are performed [9].

Experimental section

A silane coupling agent comprises three parts related to different functionalities:

| II Rubber compound formulations | | | | | | | | | | | | | | | | | | | | |
|---------------------------------|-------------|-----------|----------|------------|----------|----------|------------|-------------|-------------|------------|--------------|--------------|----------|----------|----------|-----------|--------------|--------------|-------------|--------------|
| Ingredient | Sample code | | | | | | | | | | | | | | | | | | | |
| | TESPT 7 | TESPT 9.5 | TESPT 12 | TESPT 14.4 | DMESPT 5 | DMESPT 7 | DMESPT 8.5 | DMESPT 10.4 | TESPDeT 9.5 | TESPDeT 13 | TESPDeT 16.8 | TESPDeT 20.5 | TESH 5.3 | TESH 7.3 | TESH 9.3 | TESH 11.3 | SSA80/115phr | SSA195/65phr | SSA80/80phr | SSA195/80phr |
| S-SBR | 103 | 103 | 103 | 103 | 103 | 103 | 103 | 103 | 103 | 103 | 103 | 103 | 103 | 103 | 103 | 103 | 103 | 103 | 103 | 103 |
| BR | 25 | 25 | 25 | 25 | 25 | 25 | 25 | 25 | 25 | 25 | 25 | 25 | 25 | 25 | 25 | 25 | 25 | 25 | 25 | 25 |
| Silica (1165MP) | 80 | 80 | 80 | 80 | 80 | 80 | 80 | 80 | 80 | 80 | 80 | 80 | 80 | 80 | 80 | 80 | | | | |
| Silica (1085 GR) | | | | | | | | | | | | | | | | | 115 | | 80 | |
| Silica (1200 MP) | | | | | | | | | | | | | | | | | | 65 | | 80 |
| TESPT | 7 | 9.5 | 12 | 14.4 | | | | | | | | | | | | | 5 | 7 | 3,4 | 8,3 |
| DMESPT | | | | | 5 | 7 | 8.5 | 10,4 | | | | | | | | | | | | |
| TESDeT | | | | | | | | | 9,5 | 13 | 16.8 | 20,5 | | | | | | | | |
| TESH | | | | | | | | | | | | | 5,3 | 7,3 | 9,3 | 11,3 | | | | |
| TDAE | 5 | 5 | 5 | 5 | 5 | 5 | 5 | 5 | 5 | 5 | 5 | 5 | 5 | 5 | 5 | 5 | 5 | 5 | 5 | 5 |
| Zinc oxide | 2,5 | 2,5 | 2,5 | 2,5 | 2,5 | 2,5 | 2,5 | 2,5 | 2,5 | 2,5 | 2,5 | 2,5 | 2,5 | 2,5 | 2,5 | 2,5 | 2,5 | 2,5 | 2,5 | 2,5 |
| Stearic acid | 2,5 | 2,5 | 2,5 | 2,5 | 2,5 | 2,5 | 2,5 | 2,5 | 2,5 | 2,5 | 2,5 | 2,5 | 2,5 | 2,5 | 2,5 | 2,5 | 2,5 | 2,5 | 2,5 | 2,5 |
| 6PPD | 2 | 2 | 2 | 2 | 2 | 2 | 2 | 2 | 2 | 2 | 2 | 2 | 2 | 2 | 2 | 2 | 2 | 2 | 2 | 2 |
| TMQ | 2 | 2 | 2 | 2 | 2 | 2 | 2 | 2 | 2 | 2 | 2 | 2 | 2 | 2 | 2 | 2 | 2 | 2 | 2 | 2 |
| Sulfur | 1,4 | 0,8 | 0,24 | 0 | 1,8 | 1,2 | 0,8 | 0,4 | 1,5 | 1 | 0,4 | 0 | 3,1 | 3,1 | 3,1 | 3,1 | 1,8 | 1,4 | 2,2 | 1,0 |
| TBBS | 1,7 | 1,7 | 1,7 | 1,7 | 1,7 | 1,7 | 1,7 | 1,7 | 1,7 | 1,7 | 1,7 | 1,7 | 1,7 | 1,7 | 1,7 | 1,7 | 1,7 | 1,7 | 1,7 | 1,7 |
| DPG | 2 | 2 | 2 | 2 | 2 | 2 | 2 | 2 | 2 | 2 | 2 | 2 | 2 | 2 | 2 | 2 | 2 | 2 | 2 | 2 |

| III Ingredient specifications | | |
|-------------------------------|--|---|
| Ingredient | Specification | Supplier |
| S-SBR | Solution Styrene-Butadiene Rubber | Buna VSL 5025-2 HM Lanxess, Leverkusen, Germany |
| BR | Butadiene Rubber | Kumho KBR Seoul, S-Korea |
| Silica (1165MP) | Precipitated silica with CTAB SSA* = 160 m ² /g | Rhodia Silices, Lyon, France |
| Silica (1085 GR) | Precipitated silica with CTAB SSA* = 80 m ² /g | Rhodia Silices, Lyon, France |
| Silica (1200 MP) | Precipitated silica with CTAB SSA* = 195 m ² /g | Rhodia Silices, Lyon, France |
| TESPT | Bis-(triethoxysilylpropyl)tetrasulfide | Evonik GmbH, Essen, Germany |
| TDAE | Treated Distillate Aromatic Extract oil, ENERTHENE 1849 F | Hansen & Rosenthal, Hamburg, Germany |
| Zinc oxide | Inorganic oxide | Sigma Aldrich, St. Louis, United states |
| Stearic acid | Organic acid | Sigma Aldrich, St. Louis, United states |
| 6PPD | Antiozonant N-phenyl-N'-1,3-dimethylbutyl-p-phenylenediamine | Flexsys Brussels, Belgium |
| TMQ | Antioxidant 2,2,4- trimethyl-1,2-di-hydroquinoline | Flexsys Brussels, Belgium |
| Sulfur | Elemental sulfur, purified by sublimation | Sigma Aldrich, St. Louis, United state |
| TBBS | Accelerator N-tert-butylbenzothiazole-2-sulphenamide | Flexsys, Brussels, Belgium |
| DPG | Accelerator diphenyl guanidine | Flexsys, Brussels, Belgium |

* Specific Surface Area measured by using Cetyltrimethylammonium Bromide

A. Alkoxysilane: coupling to the silica;
B. Sulfur-moiety: coupling to the polymer;
C. Linker: hydrocarbon group for better compatibility with the polymer.
The basic requirement for the variations of the silane structure used in this study was that only one of the above-mentioned functionalities is modified, while the other parts are similar to the refer-

ence silane. The structure of the reference silane is shown in Table I/I.

In order to investigate the influence of the silane modifications on wet skid as well as rolling resistance, three different silanes were synthesized. In the first modification, two ethoxy groups out of three were replaced by inert methyl groups. This modification leads to a situation in

which only one group can bind to the silica surface on each side of the silane molecule: bis-(dimethylethoxysilylpropyl)tetrasulfide (DMESPT). The structure of this coupling agent is shown in Table I/II. For the third silane, sulfur atoms were eliminated from the reference silane: Table I/III, hence the polymer-filler interactions were limited to physical interactions: bis-(triethoxysilyl)hexane (TESH). In the fourth silane as shown in Table I/IV, the length of the aliphatic linker between the silyl- and the sulfur-moieties is increased from propyl to decyl: bis-(triethoxysilyldecyl)tetrasulfide (TESDeT). This modification should result in a better hydrophobation of the silica surface due to the longer hydrocarbon chain in the molecule and a more flexible rubber-filler interphase, but the chemical bonding to the polymer should remain unchanged. The silane coupling agent TESPT was commercially obtained from Evonik GmbH; DMESPT, TESH and TESDeT were synthesized according to a general procedure for sulfidic silane preparation [10].

A test compound containing silica Zeosil 1165 MP which is typically used in the tire industry according to the well-known green tire recipe was used [11]. In order to investigate the nature of the phenomena related to the modification of the silane structure, additionally four other batches containing Zeosil 1085 GR and Zeosil 1200 MP, differing in specific surface area, were prepared. The compound formulations are shown in Table II. A detailed specification of all ingredients is shown in Table III.

All silanes were applied at four different concentrations equimolar to the re-

| IV Mixing procedure | |
|--|--|
| Stage I | |
| Rotor speed: 110 RPM Initial temp.: 50 °C | |
| Timing (Min. sec.) | Ingredient |
| 0.00 | Add polymers |
| 1.00 | Add ½ silica, ½ silane, ZnO + stearic acid |
| 2.30 | Add ½ silica, ½ silane, oil, TMQ, 6PPD |
| 3.00 | Sweep |
| 4.00 | Dump @ ~ 155 °C |
| Stage II | |
| Rotor speed: 130 RPM Initial temp.: 50 °C | |
| Timing (Min. sec.) | Ingredient |
| 0.00 | Add I stage batch |
| 3.00 | Dump @ ~ 155 °C |
| Curatives addition | |
| Rotor speed: 75 RPM Initial temp.: 50 °C | |
| Timing (Min. sec.) | Ingredient |
| 0.00 | Add II stage batch |
| 1.00 | Add curatives |
| 3.00 | Dump @ ~ 100 °C |

ference silane and with sulfur adjustment. The TESPT content was adjusted for the first and reference compound according to the CTAB specific surface area of the silica type by using the empirical equation proposed by L. Guy: Equation 1 [12]. The amount of free sulfur added together with the curatives for all compounds was adjusted to keep the total molar amount including the sulfur contained in the coupling agent at a constant level in all batches.

$$TESPT (phr) = 5,3 \times 10^{-4} \times (CTAB)_{silica} \times (phr)_{silica} \quad \text{Equation 1}$$

To prepare the compounds, an internal laboratory mixer, Brabender 350 S with mixing volume of 390 cm³, was used. The mixing procedure is specified in Table IV. The total volume of each batch was adjusted to a fill factor of 70%. Preparation of sheets for testing was done on a two roll mill (Schwabenthan). The samples were cured in a Wickert press WLP 1600 at 160 °C to sheets with a thickness of 2 mm according to their t90 optimum vulcanization times as determined in a Rubber Process Analyzer RPA 2000 from Alpha Technologies.

Methods

Rolling resistance was assessed by measurements of the tan δ value at 60 °C and 6 % strain, measured on the Rubber Process Analyzer (RPA 2000) [13].

A Laboratory Abrasion Tester 100 (LAT 100) was used to estimate the wet skid resistance of the tire treads in conditions which better reflect the real conditions on the road; see Figure 1 [14]. Wheel samples were made by compression molding in a special mold using the Wickert laboratory vulcanization press. Testing was performed at five different water temperatures: 2 °C, 8 °C, 15 °C, 22 °C, 30 °C, and at a constant slip angle of 15°. An electro-corundum disc with relative roughness of 180 was used to simulate tire-road interactions. Tests were performed at constant speed of 1.5 km/h and a load of 75 N for a distance of 33 meters. The Side Force Coefficient (SFC) values: Equation 2, for the particular samples are compared with the reference value obtained for the sample TESPT 7 and given as relative values. The given property with higher rating is always better.

$$Sfc = \frac{F_y}{F_z} \quad \text{Equation 2}$$

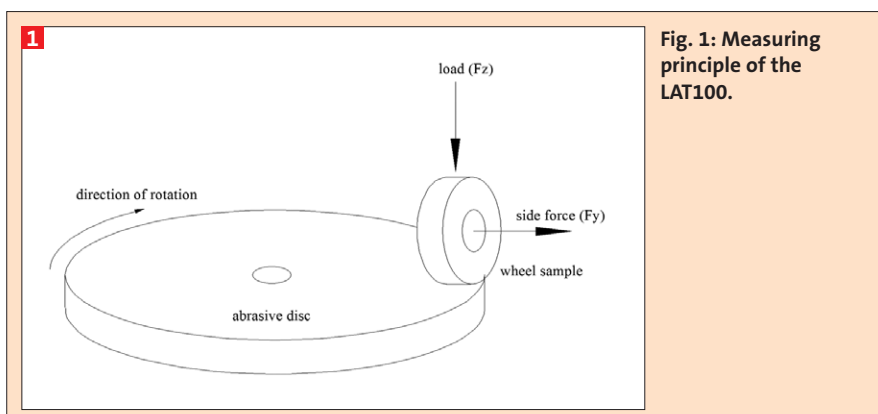


Fig. 1: Measuring principle of the LAT100.

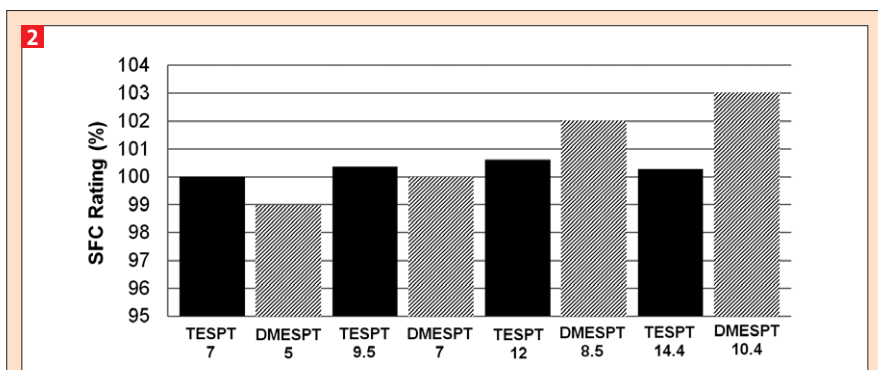


Fig. 2: Correlation between side force coefficient and silane concentration as an indication for wet skid resistance for DMESPT and TESPT containing compounds.

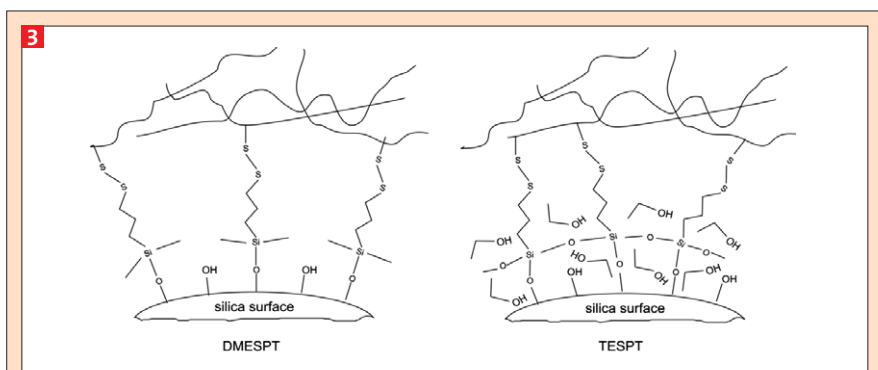


Fig. 3: Pictorial view of the silica surface after treatment with TESPT and DMESPT.

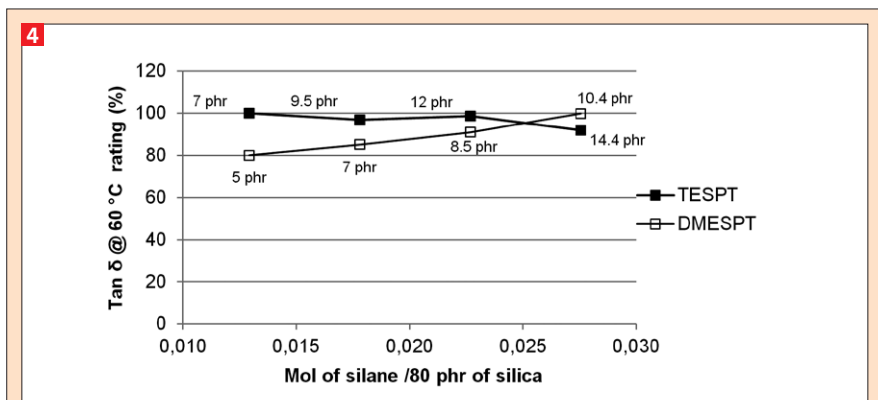


Fig. 4: Differences in tan δ values at 60 °C as indication of rolling resistance for the triethoxysilane (TESPT) and monoethoxysilane (DMESPT) containing compounds.

Where F_y and F_z are the applied load and side force respectively, as measured during testing; see Figure 1.

The dynamic mechanical analysis was performed in tension mode on a Metravib DMA2000 dynamic spectrometer.

The samples were cut from the cured sheets of the rubber compounds. For producing dynamic curves, measurements were performed at temperatures between -50°C and 80°C at a dynamic strain of 0.1% and a frequency of 10 Hz.

Results and discussion

Influence of number of alkoxy groups reacting with silanol groups on the filler surface

Unlike for TESPT, for DMeSPT the SFC as indicator for wet skid resistance is dependent on the silane concentration within the range of this study, as seen in Figure 2. This can be explained by the differences in structure of the two silanes, and as a consequence of the different degree of hydrophobicity of the silica after silanization. Before the reaction with a silane, the silica surface is covered with silanol groups; dependent on the analysis technique there may be up to 7 SiOH-groups per square nanometer of the silica surface [15]. In the case of TESPT, saturation of the silica surface with silane molecules occurs early: TESPT carries three ethoxy groups on each silicone atom. The molecule of TESPT reacts with the silica surface in a stepwise manner: one ethoxy group reacts first: the primary reaction; then lateral groups can react with themselves leaving some unreacted silanol groups: the secondary reaction as illustrated in Figure 3 on the right hand side. In the case of DMeSPT, only one ethoxy group is present which can react with a silanol group. In actual practice, not all three ethoxy groups of TESPT will react, but nevertheless remaining ethoxy groups sterically hinder attachment of silane molecules onto neighboring silanol groups. The hydrolysis rate of the primary silanization reaction, which is the reaction of the first ethoxy group, is substantially higher ($k = 0,122 \text{ min}^{-1}$) than the rate of the secondary reaction ($k = 0,008 \text{ min}^{-1}$) [16,17]. Hence in the case of TESPT, there is still a substantial number of unreacted lateral ethoxy groups after the primary silanization reaction, which occurs during mixing. During the vulcanization stage under the influence of high temperatures, these lateral ethoxy groups can further condensate and generate ethanol, which acts as an interface plasticizer, as shown in Figure 3. In the case of TESPT, rearrangement or desorption of the polymer chains at such a "soft" filler-polymer interphase is relatively easier than for DMeSPT. Lack of the lateral ethoxy groups in the case of DMeSPT blocks this silane from undergoing a secondary silanization reaction, which leads to a stiffer polymer-filler interphase, see Figure 3 on the left hand side.

The stiffer filler-polymer interphase in case of DMeSPT also results in a positive effect on WSR. Micro-asperities existing

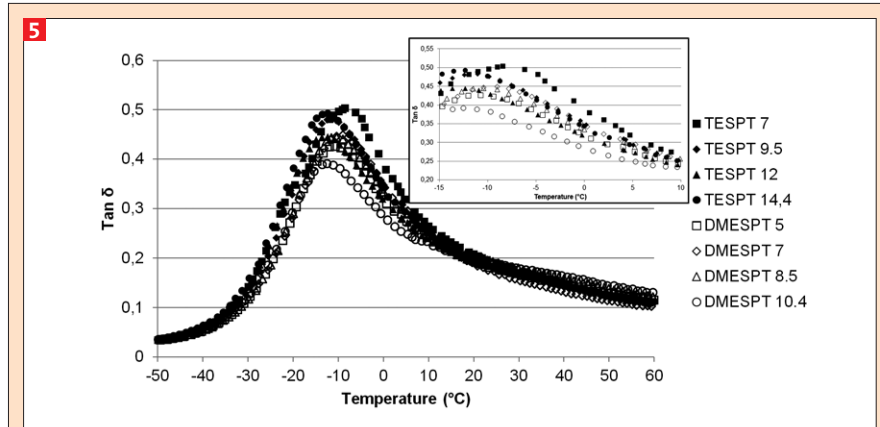


Fig. 5: Tan δ versus temperature measured at 1% of static and 0.1% of dynamic strain for the compounds containing different concentrations of TESPT and DMeSPT.

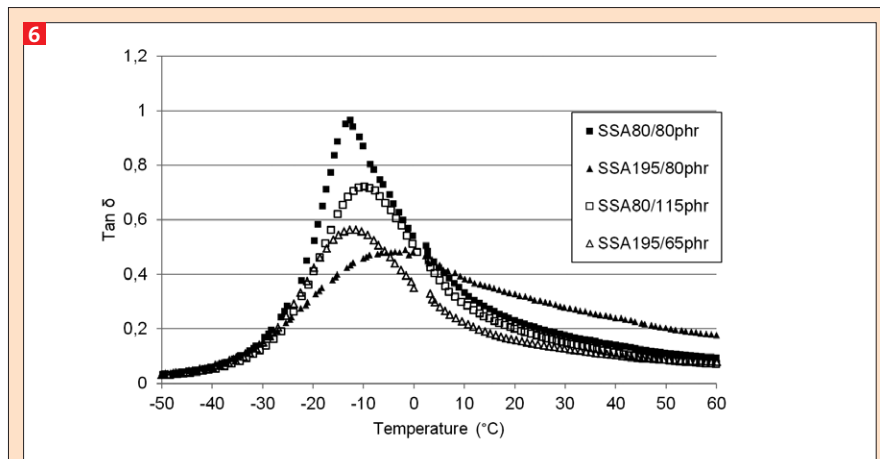


Fig. 6: Tan versus temperature measured at 1% of static and 0.1% of dynamic strain for the compounds containing two silica types differing in CTAB surface area. For instance SSA 80/80 p/hr means that the compound was loaded with 80 p/hr of silica with a specific surface area of $80 \text{ m}^2/\text{g}$.

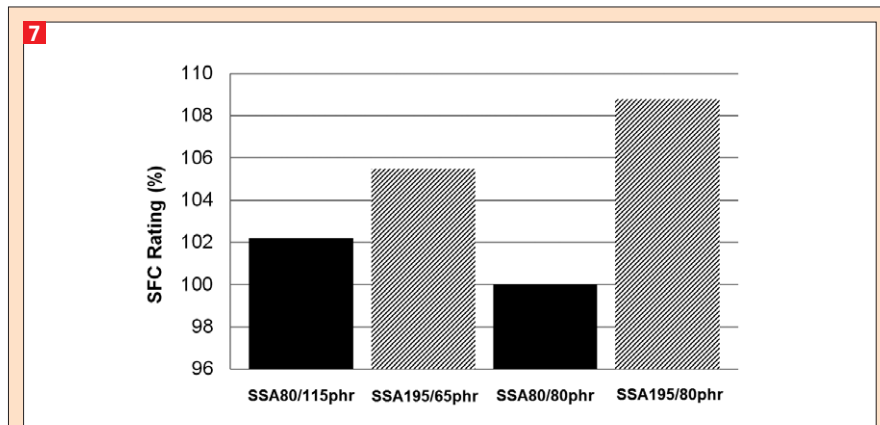


Fig. 7: Side force coefficient for the silicas with different CTAB surface area.

on the surface of the road, or equally on the abrasive disk in the LAT 100 test, cause high strain deformations on micro scale. The stiffer the interface between filler surface and elastomer, the higher the force required for this deformation. Hence, a higher local stiffness around the filler particles with high DMESPT concentrations results in higher wet skid resistance as seen in Figure 2.

The rating of the $\tan \delta$ at 60 °C as indicator of rolling resistance is shown in Figure 4. With a rising amount of DMESPT, the values of $\tan \delta$ at 60 °C increase: With an increasing loading of DMESPT, a higher concentration of unreacted silane is expected. This unreacted silane condenses further, what finally leads to the generation of ethanol at the silica surface like in the case of TESPT, but to a lower extent. Due to the scorchiness of the sample, a decrease of the $\tan \delta$ value is observed for the highest TESPT loading of 14.4 phr. Two effects might occur here: Polymer network formation, increasing the elasticity of the material, and oligomerization of the silane.

When equimolar concentrations of both silanes are compared, the hysteresis of the compounds containing the monoethoxy silane decreases relatively to TESPT in the lower temperature range, as can be seen in Figure 5. This behavior is comparable to what is observed when silicas with different specific surface areas are used: Silica with a higher specific surface area reduces the height of the $\tan \delta$ peak and is also characterized by higher values of the side force coefficient, as illustrated in Figures 6 and 7. In this series of experiments, the silica concentration was adjusted for equal hardness, and an additional outcome was similar filler-filler interactions measured by the Payne effect [18], expressed as the difference between the values of storage modulus (G') measured at low and high strain amplitudes.

The effect of reduced height of the $\tan \delta$ peak is caused by more restricted movements of the polymer chains on the surface of the silicas characterized by higher specific surface area. The same effect of decreasing height of the $\tan \delta$ peak is also observed when silica or carbon black filled rubber is compared with unfilled one [19-21]. Based on these different studies, it can be concluded that the maximum of the $\tan \delta$ graph at glass transition is decreasing in height with increasing filler-polymer interactions. As this is observed here as well when replacing TESPT by DMESPT, this supports the

assumption of more restricted polymer chain movements in the interphase between polymer and filler surface in case of DMESPT.

Influence of length of the linker between filler and polymer

A pictorial view of the silica surface modified with TESDeT is shown in Figure 8. Since the decyl linker is much longer, it is also more flexible than the propyl linker

of TESPT, and it can actually fold on the surface of silica forming more shell-like structures around the silica particles. Increasing the length of the aliphatic linker from 3 to 10 carbon atoms does not show a clear trend for the side force coefficient as seen in Figure 9. However, it does cause a substantial drop in $\tan \delta$ at 60 °C as shown in Figure 10.

At higher temperatures and strain levels, typical for a rolling tire, the long

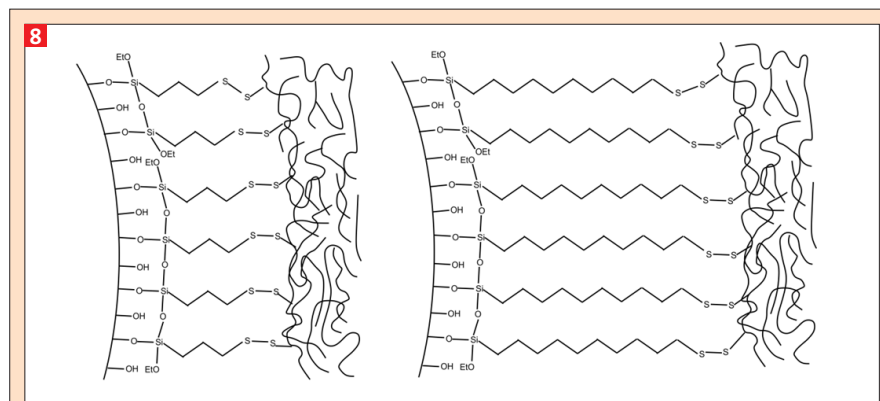


Fig. 8: Pictorial structure of TESDeT on the silica surface.

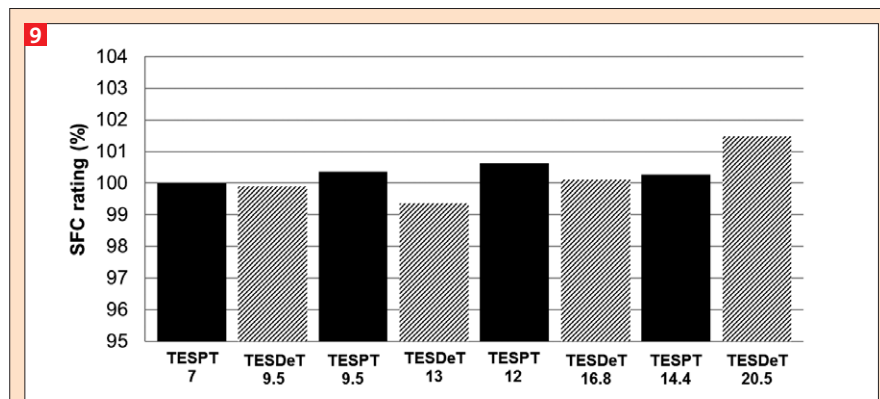


Fig. 9: Side force coefficient as measurement of the wet skid resistance versus concentration of TESDeT and TESPT.

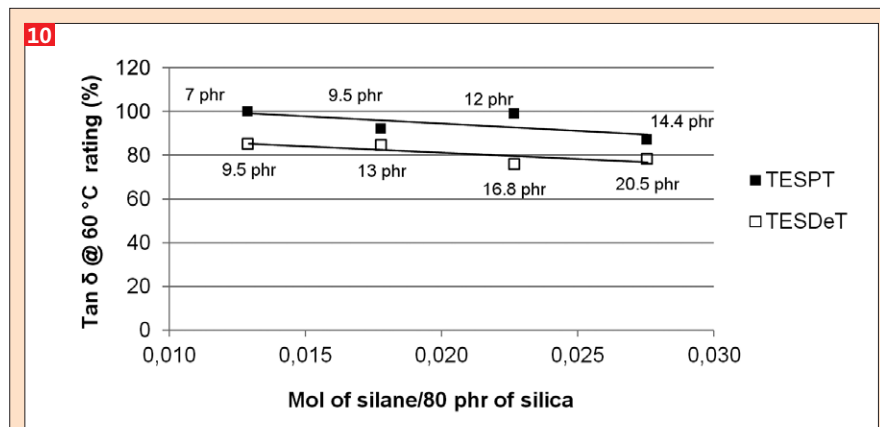


Fig. 10: Tan δ at 60 °C as indication of rolling resistance of the samples containing TESDeT and TESPT.

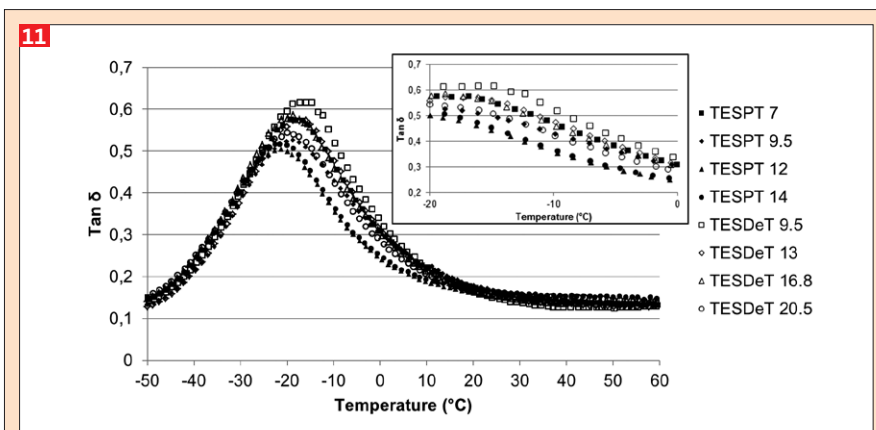


Fig. 11: Tan δ vs. temperature dependence measured at 1% of static and 0.1% of dynamic strain for the compounds containing TESPT and DMeSPT.

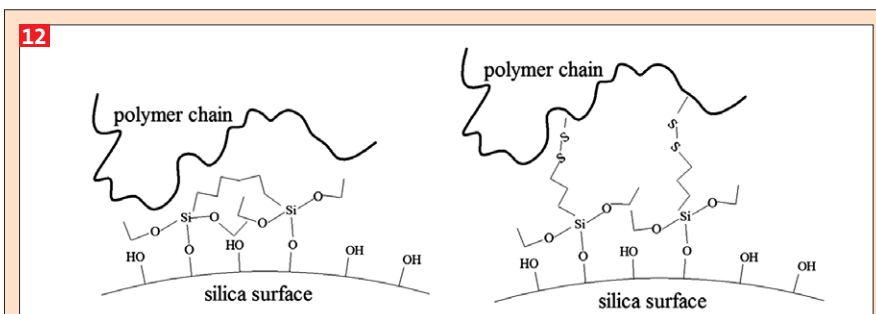


Fig. 12: Pictorial view of the silica surface after modification with TESH (left) and TESPT (right).

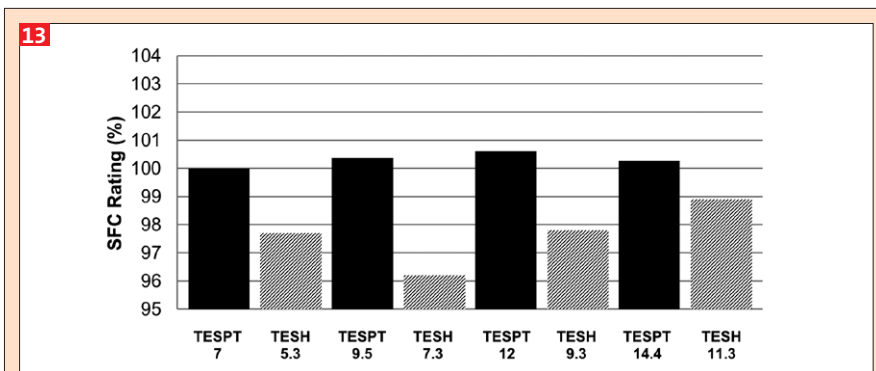


Fig. 13: Differences in side force coefficient for different loadings of TESH and TESPT as indication for wet skid resistance.

linker acts like a “jelly” shell around the silica particles. Due to the flexibility of the linker, it can accommodate higher strain amplitudes occurring during rolling within the filler-polymer interphase. The polymer network by itself therefore transfers energy more efficiently in the case of TESDeT as coupling agent, at higher temperatures typical for rolling resistance. Short, more rigid filler-polymer bonds like in the case of TESPT lead to a polymer shell around silica particles in which the polymer movements are more restricted.

At lower temperatures, the replacement of TESPT by TESDeT leads to increased energy dissipation, see Figure 11. This behavior is comparable to the effect observed when the silica with low specific surface area is used as filler, as seen in Figure 6. The same trend is also observed when the filler content is reduced [19]. It indicates that a longer linker leads to less restricted polymer movements in the silica surface - polymer interphase like in the case of silica with low specific surface area. Less restricted movements of the polymer chains mean that a higher number of poly-

mer chains can contribute to energy dissipation at lower temperatures. This consumes extra energy leading to the increase in hysteresis peak at glass transition.

By replacing TESPT with a silane with a longer linker, the rolling resistance of this material in a tire tread can be improved. However, the major drawback of TESDeT is its high molecular weight: in order to obtain equimolar concentrations, much higher amounts of TESDeT need to be applied compared to TESPT.

Influence of bond strength between coupling agent and polymer

A filler that is weakly connected to the polymer by lack of chemical bonding as sketched in Figure 12 on the left hand side, may cause sliding of the polymer on its surface during loading-unloading cycles, increasing the energy lost during rolling. Lack of chemical coupling of the filler to the polymer indeed results in an increase in rolling resistance, Figure 14, as well as in a drop in wet skid resistance as seen in Figure 13. This implies that simple hydrophobation of the silica surface without chemical filler-polymer bonding is not sufficient to obtain good wet skid and rolling resistance.

The dependence of the tan δ on temperature for the various compounds is shown in Figure 15. In general, the TESH containing compounds have lower values of tan δ in the lower temperature range compared with the TESPT containing compounds, while replacing TESPT with TESH shifts the curves towards higher temperatures. An explanation for the shift of the tan δ peak could be differences in the polymer crosslink density as a consequence of the higher sulfur loading in the case of TESPT. However, the values of the crosslink densities measured for the samples containing TESPT and TESH are similar; not further specified in this context. Hence this explanation does not apply in here.

The position of the tan δ peak on the temperature axis may also be related to filler-filler interactions, as can be derived from the comparative study of silica types differing in specific surface area. The graphs shown in Figure 6 show the results of two compounds with equal silica loadings, which also show a significantly higher Payne effect for the high surface area silica. Thus, increased filler-filler interactions cause the tan δ peak to shift towards higher temperatures for silica with higher specific surface area. In the case of TESH the same effect is observed, which may also be interpreted as higher

filler-filler interaction; this also leads to a higher Payne effect, which was 100% higher in comparison with TESPT.

The height of the $\tan \delta$ peak decreases when TESPT is replaced by TESH. From what was observed before, this is unexpected: TESH is not able to form chemical filler-polymer bonds, and therefore may not cause the same immobilization of the polymer-filler interphase as TESPT does. However, a strong physical interaction might have the same effect, as for example seen with carbon black [18]. The polymer movements are then restricted, but this time by physical forces only.

Conclusions

The position and peak height of the $\tan \delta = f(T)$ curve is correlated to the filler-polymer and filler-filler interactions. The filler-polymer interactions determine the peak height: the more restricted the polymer movements on the filler surface, the lower the height of the peak. The filler-filler interaction determine the position of the peak on the temperature axis: increasing filler-filler interactions shift the curve to higher temperatures.

A proper choice of the coupling agent allows to adjust the dynamic properties of silica-filled rubber, which are related to tire performance. By using a silane such as TESH, which cannot form chemical bonds between silica and the polymer, wet skid as well as rolling resistance deteriorate. Increased linker length of the coupling agent as in the case of TES-DeT reduces rolling resistance significantly, but does not change wet skid resistance. Using just one ethoxy group instead of three improves both, wet skid and rolling resistance. An explanation of this improvement is a stronger filler-polymer interface due to a lower ethanol emission during the vulcanization phase.

Acknowledgements

This project is carried out in the framework of the innovation program 'GO Gebundelde Innovatiekracht', and funded by the 'European Regional Development Fund'. The project partners Apollo Tyres Global R&D, Enschede, the Netherlands, University of Twente (Tire-Road Consortium), Enschede, the Netherlands, and Elastomer Research and Testing B.V., Deventer, the Netherlands, are gratefully acknowledged for their support.

References

[1] A. A. Ward, A. A. Yehia, A. M. Bishai, *Kautsch. Gummi Kunstst.* **61** (2008) 569.

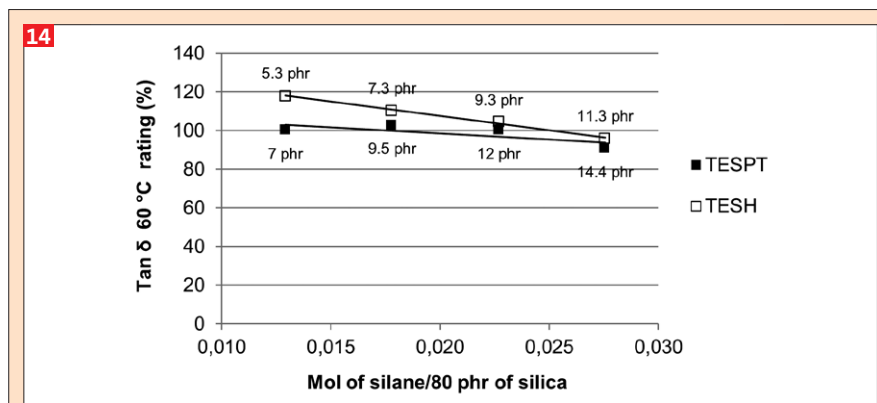


Fig. 14: Tan δ at 60 °C values as indication of rolling resistance of the samples containing TESPT and TESH.

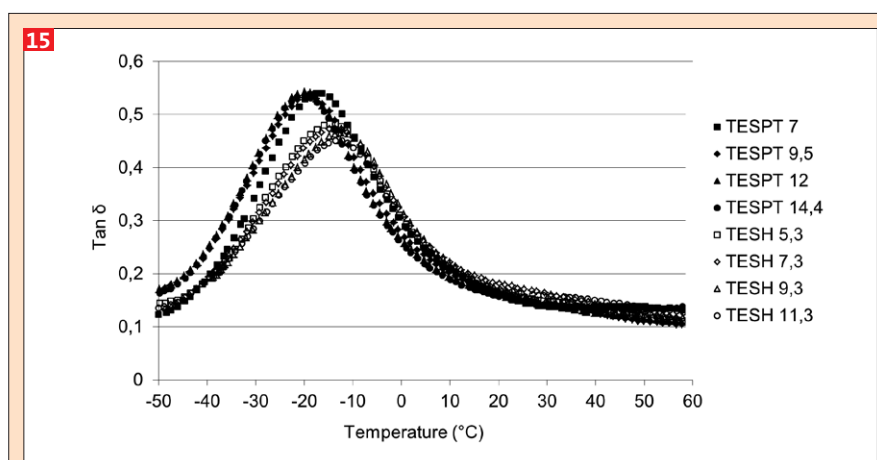


Fig. 15: Tan δ - temperature dependence measured at 1% of static and 0.1% of dynamic strain for the compounds containing TESPT and TESH.

- [2] L.A.E.M. Reuvekamp, P.J. van Swaaij, J.W.M. Noordermeer, *Kautsch. Gummi Kunstst.* **63** (2009) 35.
- [3] K.H. Nordsiek, *Kautsch. Gummi Kunstst.* **38** (1985) 177.
- [4] M. J. Wang, *Rubber Chem. Technol.* **71** (1998) 520.
- [5] A. Schallamach, "Chemistry and Physics of Rubber-like Substances" ed. L. Bateman. McLaren and Sons, London (1963) 382.
- [6] A. Yoshioka, K. Komuro, A. Ueda, H. Watanaabe, S. Akita, T. Masuda, A. Nakajima, *Pure and Applied Chemistry* **58** (1986) 1697.
- [7] S. Cerveny, A. Ghilarduccib, H. Salvab, A.J. Marzoccaa, *Polymer* **41** (2000) 2227.
- [8] M. J. Wang, *Kautsch. Gummi Kunstst.* **61** (2008) 33.
- [9] M. Heinz, K. A. Grosch, 167th Technical meeting of the Rubber Division ACS, 16-18th of May 2005, San Antonio, Texas.
- [10] J. Munzenberg, W. Will, G. Zzulka, US Patent No. 5892085 (1999), to Degussa AG.
- [11] R. Rauline, European Union Patent No. EP0501227B1 (1992), to Michelin Co.
- [12] L. Guy, Ph. Cochet, Y. Bomal, S. Daudey, *Kautsch. Gummi Kunstst.* **63** (2009) 383.
- [13] L.A.E.M. Reuvekamp, "Reactive mixing of silica and rubber for tires and engine mounts", PhD thesis: 2003, Dept. of Rubber Technology, Univ. of Twente, Enschede, the Netherlands.
- [14] M. Heinz, *Journal of Rubber Research* **13** (2010) 91.
- [15] M. J. Wang, *Rubber Chem. Technol.* **71** (1998) 520.
- [16] A. Hunsche, U. Görl, H. G. Koban, Th. Lehmann, *Kautsch. Gummi Kunstst.* **51** (1998) 525.
- [17] H. D. Luginsland, A. Hasse, 157th Technical meeting of the Rubber Division ACS, April 4 - 6th (2000) Dallas, Texas.
- [18] A. R. Payne, R. E. Whittaker, *Rubber Chem. Technol.* **44** (1971) 440.
- [19] L. Guy, Solvay-Rhodia, private communication, 2012.
- [20] M. M. Jacobi, M. V. Braun, T. L. A. C. Rocha, R. H. Schuster, *Kautsch. Gummi Kunstst.* **60** (2007) 460
- [21] M. J. Wang, *Kautsch. Gummi Kunstst.* **60** (2007) 438